Heavy Quarkonium Production at HERA

Christian Kiesling

Max-Planck-Institut für Physik (Werner-Heisenberg-Institut),
Föhringer Ring 6, D-80805 München

Abstract. In this article, recent results on electro- and photoproduction of heavy vector mesons at HERA are reviewed. Various models for the inelastic and elastic production mechanisms are discussed and confronted with the measurements. Elastic production allows comparison of two distinct theoretical concepts, i.e. the Regge ansatz and models using perturbative QCD (pQCD), where the colorless exchange is modeled by multiple gluon exchange. While production of light vector mesons is well described in the Regge picture, the heavy vector meson data show clear deviations from the universal "soft" Pomeron prediction. Perturbative QCD, however, is able to reproduce the trend of the data, as well as a more general Regge fit using an additional "hard" Pomeron.

1 Introduction

One of the most striking early results from the HERA collider was the detection of the strong rise [1,2] of the proton structure function F_2 towards low values of the Bjorken variable x. These findings could be interpreted by a dramatic increase of the gluon density within the proton and provided strong motivation to numerous subsequent measurements of the electron-protron interaction at low x and low momentum transfer Q^2. In the course of these measurements a new class of events were (re-)discovered [3,4], namely the diffractive production of hadrons, both in electroproduction and photoproduction (at HERA the latter are defined as events with an undetected electron in the final state, emitted at very small angles and exhibiting very small Q^2). A surprisingly large fraction of the produced events showed a large rapidity gap between the produced secondary hadrons and the outgoing nucleon, indicative for a color singlet exchange between the two hadronic systems. These events led to a revival of interest in Regge theory, more precisely in Pomeron exchange, which in the past could successfully describe "soft" diffractive processes in hadron-hadron and photon-hadron collisions. The correct prediction of the total cross section for quasi-real photons (γ^*) colliding with protons (p) at HERA, which entered an entirely new kinematic domain, was a clear triumph for the Pomeron exchange interpretation: Pomeron exchange is characterized by a universal trajectory, independent of the composition of the initial hadronic state, and predicts a slow rise of the total cross section with increasing hadronic center-of-mass energy $W = W_{\gamma^* p}$. Other data, such as the slowly rising cross sections for exclusive light vector meson (ρ, ω, ϕ) production, contributed to the strengthening of the "soft" Pomeron interpretation.

A severe blow against this consistent Pomeron picture came through the measurement of J/ψ photoproduction at HERA which, in contrast to ρ photoproduction and the soft Pomeron expectation, was observed to exhibit a much steeper rise[5,6] of the total cross section towards increasing W. The two above-mentioned phenomena, i.e. strong rise of F_2 towards low x and strong rise of the cross section for diffractive processes with increasing W, can however be understood within perturbative QCD (pQCD): The rise is caused by an increased gluon density inside the proton as a consequence of the Q^2 evolution predicted in pQCD.

An even more direct path towards the gluon density within the proton is offered by inelastic heavy vector meson electroproduction: At HERA, this process is dominated by photon-gluon fusion, which is tagged as such, e.g., through the presence of a J/ψ meson, originating from the fluctuation of the virtual photon emitted from the electron into a charm-anticharm quark pair. The color singlet nature of the J/ψ in the γg subprocess is ensured by the emission of a hard gluon in the final state (inelastic reaction) or by emission of a soft gluon re-absorbed by the partonic constituents of the proton.

All these processes, involving heavy vector meson production at HERA, are extremely useful in the investigation of the detailed gluonic structure of the nucleon and complement nicely other analyses such as jet production or the Q^2 development of the structure function F_2.

2 Kinematics and Experimental Procedures

Figure 1 shows the lowest order Feynman diagram for inelastic J/ψ production, where also the kinematics of the reaction can be defined. The process is photon-gluon fusion, where the (virtual) photon γ^* with four-momentum q is emitted from the incoming electron (or positron) of four-momentum k, and the gluon is radiated off the constituents of the proton, the four-momentum of which is p_p. Besides the mass squared of the produced vector meson M_V^2, two other scales exist in the process, relevant for the subsequent discussions: The photon virtuality $Q^2 = -q^2$ and the momentum transfer squared $t = (p_p - p_X)^2$ at the lower ("proton") vertex.

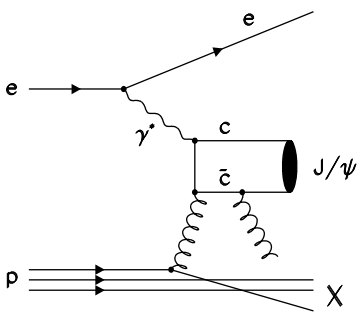

Fig. 1. Feynman diagram for inelastic vector meson (e.g. J/ψ) production as a boson gluon fusion process. The following four-vectors define the kinematics: incoming proton p_p, incoming electron k, scattered electron k', exchanged photon $q = k - k'$, outgoing vector meson p_V. The hadronic center-of-mass energy W is given by the virtual photon, emitted from the electron, and the incoming proton: $W^2 = (p_p + q)^2$
.

The energy y of the virtual photon, in units of the electron energy in the proton rest system, is given by

$$y = \frac{q \cdot p_p}{k \cdot p_p} \ . \tag{1}$$

The produced (heavy) vector meson V is emitted with energy fraction z ("elasticity") relative to the incident photon energy fraction y in the proton rest system, which is given by

$$z = \frac{p_p \cdot p_V}{p_p \cdot q} = \frac{E_V}{E_\gamma} \ . \tag{2}$$

The variable z can be used to separate photon-gluon fusion from resolved photon processes, which dominate for $z < 0.2$ [7]. For elastic reactions, no hard gluon is radiated and the hadronic system X is just the proton. In this limit the vector meson's elasticity z approaches unity: $z \approx 1$.

In order to measure the reaction $\gamma^* p \to VX$, both H1 and ZEUS require the heavy vector meson V to be detected essentially in the central detector (H1 also uses the backward electromagnetic calorimeter to detect J/ψ mesons decaying into electron-positron pairs). One can distinguish the following reactions producing a heavy vector meson in the final state:

- *inelastic production*: The vector meson is produced accompanied by additional hadrons from the hard gluon (see fig. 1). The initial proton at the lower vertex is transformed to a general hadronic state X. Typically, the elasticity for the J/ψ is small, $z \leq 0.9$ but larger than about 0.2 in order to exclude background where the meson V is produced in the fragmentation chain of a quark- or gluon-initiated jet.
- *dissociative production*: The vector meson is produced "elastically" (no hard gluon in the final state), but the proton dissociates into a state X with $M_X > M_p$ and $z \leq 1$.
- *elastic (exclusive) production*: The vector meson is produced truly elastically and the proton stays intact, $z \approx 1$.

3 Theoretical Concepts of Heavy Quarkonium Production

Electro- and photoproduction of vector mesons $V(= \rho, \omega, \phi, J/\psi, \Upsilon)$, i.e. $ep \to eXV$, provides a wealth of information on the properties of the strong interaction. As indicated schematically in fig. 1, one of the motivations for the study of inelastic production of vector mesons is the possibility to directly probe the gluon content in the nucleon. Processes such as exclusive vector meson production ($ep \to epV$), on the other hand, may be used as sensitive tools to study soft and hard diffractive processes and the hadronic structure of the virtual photon. While perturbative QCD is expected to describe inelastic vector-meson production - given a sufficiently large scale in the scattering process - there are two major theoretical concepts for the description of the diffractive reactions, i.e. Regge phenomenology and, again, perturbative QCD.

3.1 Regge Models

High energy hadron-hadron and photon-hadron scattering display many features characteristic for optical diffraction, among them total cross sections slowly rising with the hadronic center of mass energy W and a strong (exponential) drop of the elastic differential cross section $d\sigma/dt$ away from the forward direction. Donnachie and Landshoff[8] have found an extremely simple parameterization of the energy dependence of all the total and differential cross sections at high energies, based on the exchange of a particular Regge trajectory[9], the so-called Pomeron (P) trajectory $\alpha_{\rm P}$, defined by two parameters:

$$\alpha_{\rm P}(t) = \alpha_{\rm P}^0 + \alpha'_{\rm P}\, t \ . \tag{3}$$

The differential cross section $d\sigma/dt$ for elastic scattering processes at low values of $|t|$ is well described by a single exponential in t with a slope parameter, varying in a characteristic manner with the energy W:

$$\frac{d\sigma}{dt} \propto e^{-b|t|} \quad , \quad b = b_0 + 2\alpha'_{\rm P} \ln\left(\frac{W^2}{W_0^2}\right) \ . \tag{4}$$

Here, b_0 and W_0 are process-dependent constants. Using the optical theorem, the total cross section is then given by

$$\sigma(W) \propto \frac{W^{4(\alpha_{\rm P}^0-1)}}{b} \sim W^{0.22} \ , \tag{5}$$

where the numerical value in the exponent of W results from $\alpha_{\rm P}^0 = 1.08$ and $\alpha'_{\rm P} = 0.25{\rm GeV}^{-2}$, which have been determined from fits to all available total cross section data[8].

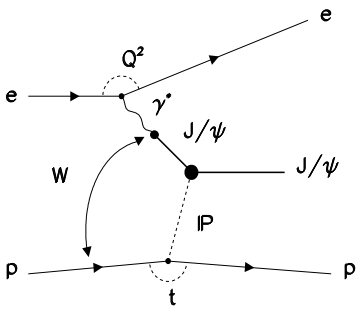

Fig. 2. Feynman diagram for elastic vector meson (e.g. J/ψ) production within the framework of Regge phenomenology, exhibiting vector-meson dominance and Pomeron exchange. In electroproduction, the hadronic center of mass energy W is given by the virtual photon, emitted from the electron, and the incoming proton.

In the framework of Regge phenomenology, electroproduction of vector-mesons is viewed as a two-step process as indicated in fig. 2: First, the (virtual) photon emitted from the electron fluctuates into a vector meson, described by the Vector-Meson Dominance model (VDM[10]), and the vector meson in turn scatters elastically off the proton, exchanging Reggeons like "ordinary" hadron-hadron

interactions. Based on this picture, the following predictions are made: The total cross section for $\gamma^* p \to pV$ at high virtual-photon proton energy W rises slowly with W, no additional dependence on the photon virtuality Q^2 is expected concerning the rise of cross section with W. The differential cross section is falling exponentially with t, the slope parameter b increasing logarithmically with W, driven by $\alpha'_{\mathrm{P}} = 0.25$ GeV^{-2}[8]. This feature of the differential cross section is called "shrinkage": due to the increasing b the differential cross section steepens with energy, the diffractive forward peak becomes narrower, or "shrinks". A further prediction of the Regge model is the complete transfer of the photon helicity to the final state vector meson (s-channel helicity conservation, SCHC). SCHC can be tested analyzing the angular distribution of the decay particles in the rest frame of the vector meson.

It is well-known by now that the HERA data on J/ψ photo- and electroproduction are not described by the simple ("soft") Regge model. A natural extension within the Regge phenomenology was to introduce in addition to the soft Pomeron trajectory $\alpha_{\mathrm{P}}(t)$ a "hard" Pomeron trajectory $\alpha_{\mathrm{P}'}(t)$ with suitable parameters $\alpha^0_{\mathrm{P}'}$ and $\alpha'_{\mathrm{P}'}$, so that the data can, again, be correctly described. Such an approach was recently proposed by Donnachie and Landshoff[11].

3.2 Perturbative QCD

Given a sufficiently large scale such as the photon virtuality, the momentum transfer t, or the mass of the produced vector meson, diffractive processes can be viewed as mediated, to lowest order, by an exchange of two gluons (in a color singlet state) between a quark-antiquark pair (emitted from the photon) and the constituents inside the proton (see fig. 3). In models based on pQCD

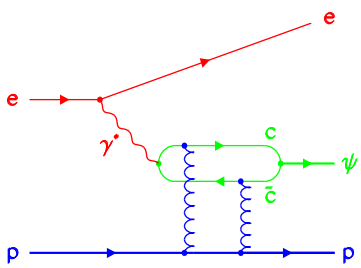

Fig. 3. Feynman diagram for elastic J/ψ production within the framework of perturbative QCD: The virtual photon couples to a $c\bar{c}$ pair and two gluons in a color singlet state are exchanged, in lowest order, between the quark pair and the proton. The $c\bar{c}$ pair forms a J/ψ with a probability derived from the bound-state wave function.

the reaction $\gamma^* p \to Vp$ (the virtual photon γ^* being radiated off an incoming electron or positron) is viewed as a temporal sequence of three sub-processes[12]: First the virtual photon γ^* fluctuates into a $q\bar{q}$ pair, which then scatters off the proton target exchanging, in lowest order, a color singlet two-gluon system or, more generally, a gluon ladder. Finally the $q\bar{q}$ pair turns into a vector meson. Elastic (heavy) vector meson production may thus be used as an alternative way to probe the gluon content of the proton[13]. While in [12] only the case of high Q^2 is considered, where the longitudinal components of the virtual photon and

the produced vector meson are supposed to dominate, several authors[14–16] have generalized this model to include also transversely polarized photons and vector mesons, and heavy vector meson photoproduction, the calculations being carried out in leading order (LO) $\alpha_S \ln(Q^2/\Lambda^2_{QCD})$. The calculations of Frankfurt et al.[15] yield the following prediction for the forward differential cross section (the Ryskin formula[16] is similar):

$$\left.\frac{d\sigma^{\gamma^* p}}{dt}\right|_{t=0} = \frac{12\pi^3 \Gamma_{ll} M_V^3}{\alpha_{em}(Q^2+4m_c^2)^4} \cdot \left|\alpha_S(\tilde{Q}^2)\left(1+\frac{i\pi}{2}\frac{d}{d\ln x}\right) x g(x,\tilde{Q}^2)\right|^2 \cdot \left(1+\epsilon\frac{Q^2}{M_V^2}\right)\mathcal{C}(Q^2)\ . \tag{6}$$

In this expression, ϵ is the flux ratio of longitudinally to transversely polarized incoming virtual photons, given by

$$\epsilon = \frac{\Gamma_L}{\Gamma_T} = \frac{1-y}{1-y+y^2/2}\ . \tag{7}$$

At HERA, ϵ is very close to unity. The function $\mathcal{C}(Q^2)$ is related to the vector meson's wave function and approaches unity from below for $Q^2 \to \infty$. The momentum fraction x_g carried by the gluon is given by

$$x_g \approx \frac{Q^2+M_V^2}{W^2}\ . \tag{8}$$

The main uncertainties in these calculations for J/ψ production come from relativistic effects in the vector meson wave function (Fermi motion of the charmed quarks) and from the uncertainty of the charm quark mass. In the model of Ryskin the effective scale is $\tilde{Q}^2 = (Q^2+M_V^2)/4$, while it is roughly a factor of 2 larger in the Frankfurt et al. model.

As can be seen from eq. 6, pQCD makes a prediction for the forward elastic differential cross section. In order to predict the total elastic cross section, the slope parameter b (see eq. 4) needs to be known, for which no QCD prediction exists. The slope has therefore to be taken from experiment and the total cross section is determined by

$$\sigma^{\gamma^* p} = \frac{1}{b}\left.\frac{d\sigma^{\gamma^* p}}{dt}\right|_{t=0}\ . \tag{9}$$

Concerning inelastic heavy vector meson production, substantial progress has been made during the past years with the introduction of an effective field-theory framework of nonrelativistic QCD (NRQCD)[17]. In this approach the NRQCD matrix elements factorize into short-distance coefficients describing the production of a heavy quark-antiquark system, calculated using ordinary perturbative techniques, and effects from long-distance physics describing the hadronization of the quark-antiquark pair. The long-distance effects are parameterized in terms of color multiplet matrix elements (see, e.g., [18]), which can be determined from

experiment or, at least in principle, from non-perturbative calculus such as lattice QCD. In contrast to elastic vector meson production, the inelastic cross section depends linearly on the gluon density in the proton.

Compared to previous work on heavy quarkonium production employing the color singlet model (see, e.g. [19] for an extensive review), the NRQCD formalism allows for the possibility that a $c\bar{c}$ pair produced in a color octet state may evolve non-perturbatively into a J/ψ or a ψ'. Such color octet contributions were in fact successful in explaining the large J/ψ and ψ' production rates observed by the CDF and D0 collaborations[20] at the Tevatron.

4 Heavy Quarkonium Production in Deep Inelastic Scattering

The subsequent discussion of the experimental data on heavy quarkonium production will concentrate mainly on the J/ψ. We will start with inclusive production and then turn to the inelastic and exclusive channels. In order to make meaningful comparisons of the various models introduced above with the experimental data, the separation of elastic and inelastic production of vector mesons is a major experimental issue; the distinction between photoproduction and electroproduction is straightforward through the observation of the scattered electron in the final state.

4.1 Inelastic Production of J/ψ Mesons

In general, the "diffractive" and "inelastic" regimes are separated by a cut in the variable z (see eq.2). The diffractive component is expected at values of z close to unity. However, large non-diffractive contributions, most importantly color octet contributions, are expected[18] at high z as well, motivating a model independent analysis without such a cut. H1 has recently published data on inclusive J/ψ production[21] (see also [22]). The J/ψ was observed in its leptonic decay modes and the kinematic range covered was $2 < Q^2 < 80$ GeV^2 and $40 << 180$ GeV. The di-lepton mass spectra for two different regions of z are shown in fig. 4, where the inelastic component of the events was identified by a cut in the energy deposited close to the proton (forward) direction ($E_{\mathrm{fwd}} > 5$ GeV). This cut excludes the low mass excitations M_X of the nucleon and with it the elastic and most of the quasi-elastic diffractive events. The selection is, however, believed to retain the color octet contributions. It was verified by Monte-Carlo methods that this cut is equivalent to a cut $M_X > 10$ GeV. As expected, the inelastic component dominates at lower values of z (fig. 4a)), while the elastic and quasi-elastic component dominates at high z (see fig. 4b)).

The corrected differential cross sections with respect to several kinematic quantities (Q^2, transverse momentum squared $p^2_{t,\psi}$ of the J/ψ, z, y^* - the rapidity of the J/ψ in the $\gamma^* p$ center of mass system - and W) are shown in fig. 5 for the inclusive as well as the inelastic data. For comparison, the results of a NRQCD calculation[18] are given, which should describe the inelastic part of the cross

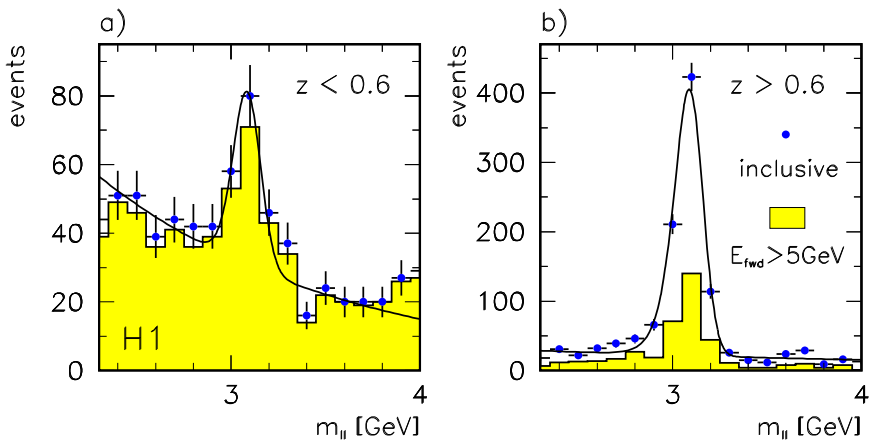

Fig. 4. Di-lepton mass spectra for events from inclusive (points) and inelastic (histogram) electroproduction of J/ψ mesons as measured in the H1 experiment[21]: a) $0.2 < z < 0.6$, b) $0.6 < z$. The curves are from fits to the signal region, convoluting a Gaussian with an exponential tail to account for radiation loss in the case of electronic decay, and an exponentially falling non-resonant background.

sections. The predictions include contributions from the color octet states $^3P_0$ and $^1S_0$, which are of order $\mathcal{O}(\alpha_S)$, and from the color singlet state $^3S_1$, which is of order $\mathcal{O}(\alpha_S^2)$. Note that both contributions are in leading order; the color singlet contribution is shown separately. The color octet contributions are found to dominate for all values of Q^2, the leading order color singlet alone falling below the data by factors 2-3. The observed differences in magnitude between predicted and measured cross sections may be indicative of the necessity to adjust the color multiplet matrix elements, determined so far from the Tevatron data alone. The differences in shape (see e.g. the y^* distribution), might be influenced by a relative adjustment of the matrix elements. Note also that a full prediction of $d\sigma/dz$ is not possible at present[18] and is therefore not shown.

One might be led to the conclusion that, like for the Tevatron data, color octet contributions seem required by the ep data, the color singlet contribution alone not being sufficient to saturate the cross sections. Still, since the calculations are only in leading order, one cannot yet claim the necessity for color octet contributions in the HERA data.

4.2 Exclusive Production of J/ψ Mesons

Both ZEUS[23] and H1[21] have recently published data on exclusive electroproduction of J/ψ mesons, $ep \to eVp$. The Q^2 (W) ranges covered are $2 < Q^2 < 80$ GeV^2 ($25 < W < 180$ GeV) for H1 and $2 < Q^2 < 40$ GeV^2 ($50 < W < 150$ GeV) for ZEUS. Exclusive production of J/ψ mesons is ensured in both experiments by requiring exactly two oppositely charged leptons in the main detector and by

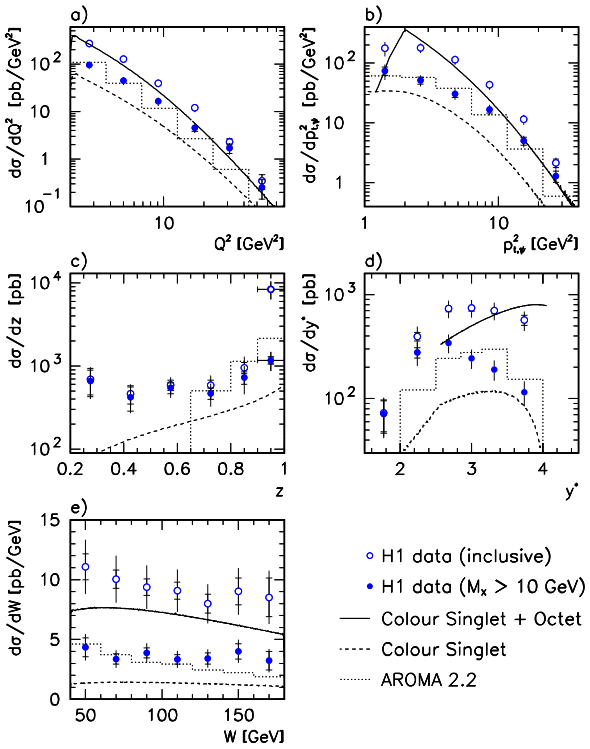

Fig. 5. Differential cross sections for the inclusive (open points) and inelastic ($M_X > 10$ GeV, full symbols) process $ep \to eJ/\psi X$ for $z > 0.2$ from H1[21]. The inner error bars are statistical, the outer bars combined statistical and systematic errors. The curves are leading order predictions for inelastic J/ψ production within the NRQCD factorization approach[18]. The histogram is from a Monte-Carlo simulation incorporating soft color interactions[24].

suppressing quasi-elastic (proton dissociation) events by requiring no activity in the forward (proton direction) parts of the detector. Residual backgrounds in the J/ψ mass region (coming mainly from low mass proton dissociation and from the Bethe-Heitler process $ep \to l^+l^-p$) are of order few percent and have been subtracted using Monte-Carlo simulations. The electroproduction cross section is converted to a virtual photoproduction cross section using

$$\frac{d^2\sigma(ep \to eJ/\psi p)}{dydQ^2} = \Gamma\sigma(\gamma^* p \to J/\psi p) \ , \tag{10}$$

where the function Γ is the flux of virtual photons[25], defined by

$$\Gamma = \frac{\alpha_{\rm em}}{2\pi y Q^2}\left(1 + (1-y)^2\right) \ . \tag{11}$$

W dependence: Figure 6 shows the resulting cross section measurements for $\gamma^* p \to J/\psi\ p$ as a function of W for various values of the momentum transfer Q^2 in the range $2 < Q^2 < 80$ GeV^2. For comparison, also the photoproduction ($Q^2 = 0$) cross sections are shown (see also below). All cross sections exhibit a steep rise with W, in contrast to the corresponding data on exclusive light vector meson production (e.g. ρ electroproduction[23,26,27]) in a similar (low) Q^2 range. Fits of the form $\sigma \sim W^\delta$ for given Q^2 yield values $\delta \approx 0.8 - 0.9$ with

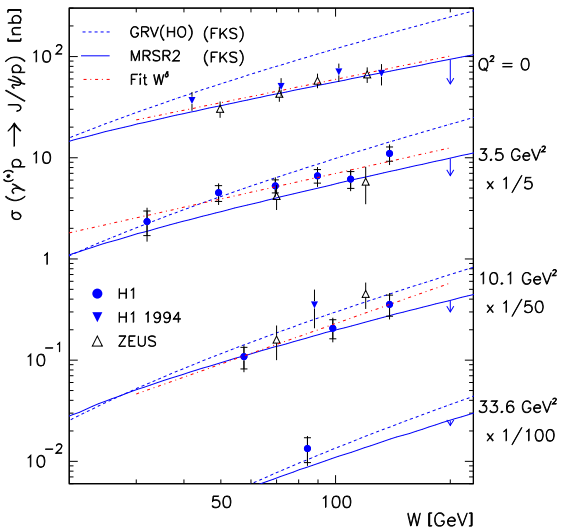

Fig. 6. Exclusive electroproduction of J/ψ mesons from H1[21] and ZEUS[23], converted to virtual photoproduction (see eq. 10) together with real photoproduction data (see discussion below). The full error bars correspond to statistical and systematic errors added in quadrature. The dashed-dotted lines result from fits of the form W^{δ}. Typical values are $\delta \approx 0.8 - 0.9$, with no significant variation with Q^2. The data are compared to various theoretical models (see text).

typical errors of about 0.2, clearly incompatible with the "soft Pomeron" slope of about 0.22 (see eq. 5). The dash-dotted lines give the results of these fits. Although in the $Q^2 = 10.1$ GeV^2 bin a somewhat large slope ($\delta = 1.3 \pm 0.4$) is measured, no significant variation of the slope with Q^2 is observed within the present precision. In addition to the phenomenological description, the full and dashed lines in the figure are results of calculations based on pQCD[15] using two different parameterizations for the gluon density inside the proton(GRV[28], MRSR2[29]). The absolute normalization of these predictions is sensitive to the mass m_c of the charm quark (see eq. 6). This is indicated in fig. 6 by the length of the little arrows denoting the change in normalization at the point $W = 200$ GeV, when m_c is changed from 1.4 to 1.5 GeV.

Q^2 dependence: The Q^2 dependence of the cross section for $\gamma^* p \to J/\psi\, p$ in the W range between 40 and 160 GeV (mean value at $W = 90$ GeV) is shown in fig. 7. At large Q^2, the naive expectation from QCD (see eq. 6) would suggest a Q^6 dependence of the cross section. However, one has to take into account the Q^2 evolution of the gluon distribution which is known to increase strongly as Q^2 grows, and the function $\mathcal{C}(Q^2)$, which both reduce the Q^2 dependence. Parameterizing the Q^2 dependence in the form $\propto (Q^2 + M_V^2)^{-n(V)}$, the J/ψ data are well described[21] by the fit with $n(J/\psi) = 2.38 \pm 0.11$. The dotted line in fig. 7 is from the pQCD model of Frankfurt et al.[15] with the MRSR2 gluon distribution, which was able to describe the W dependence of the total cross section (see fig. 6). This model also reasonably well describes the Q^2 dependence. For comparison, the cross section for $V = \rho$ is also shown in fig. 7, at somewhat lower W. Fitting the ρ data with the same Q^2 dependence yields similar values as for the J/ψ: $n(\rho) = 2.24 \pm 0.09$ from H1[26], in good agreement with ZEUS[23]

($n(\rho) = 2.32 \pm 0.10$). While the ρ dominates the cross section at low Q^2, the J/ψ approaches the ρ with increasing Q^2. At sufficiently large Q^2 ($Q^2 \gg M_V^2$), the ratio of cross sections should, according to the additive quark model, only depend on the electric charges of the $q\bar{q}$ state forming the vector meson, $\rho : \omega : \phi : J/\psi = 9 : 1 : 2 : 8$. This limit seems to be reached for $Q^2 > 20$ GeV^2. At very large Q^2 Frankfurt et al.[14] predict an enhancement of the J/ψ cross section, relative to the asymptotic quark model limit, by a factor of about 3.5. Accordingly, the J/ψ cross section would overtake the ρ cross section by such an amount. The presently accessible Q^2 range (up to 50 GeV^2) is obviously not yet high enough to test this prediction.

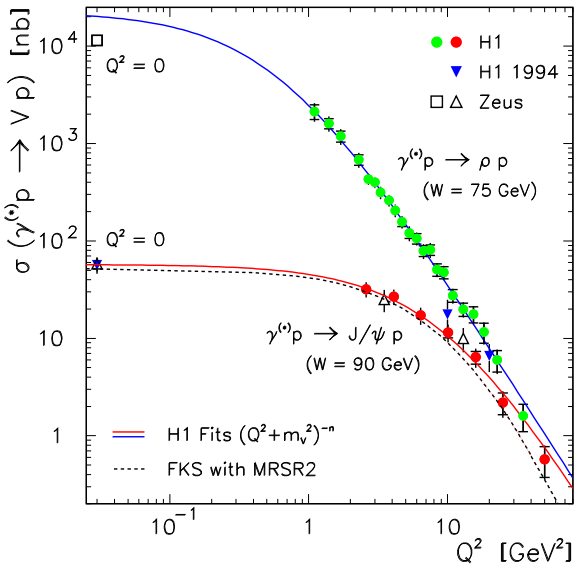

Fig. 7. Exclusive virtual-photoproduction cross sections for J/ψ ($\langle W \rangle = 90$ GeV) and ρ mesons ($\langle W \rangle = 75$ GeV) as function of the momentum transfer Q^2. The full lines are from dipole-like fits (see text) to the measurements. At large Q^2, the cross sections for ρ and J/ψ approach the SU(4) limit of 9:8. The curves are from fits of the form $(Q^2 + M_V^2)^{-n(V)}$, resulting in $n(\rho) = 2.24 \pm 0.09$[26] and $n(J/\psi) = 2.38 \pm 0.11$[21]

t Distribution: Since for electroproduction events the scattered electron is observed in the final state, the momentum transfer t can be determined unambiguously . For $|t|$ values below about 1 GeV^2 the differential cross section for elastic vector meson production can be described by a single exponential fall-off away from $|t| = 0$, characterized by the slope parameter b (see eq. 4). After correcting the experimental $|t|$ distributions for residual backgrounds (mainly from proton dissociation and the Bethe-Heitler process) H1[21] obtain $b = 4.1 \pm 0.3(\text{stat.}) \pm 0.4(\text{syst.})$ GeV^{-2} for the kinematic range $2 < Q^2 < 80$ GeV^2, $40 < W < 160$ GeV, in good agreement with the ZEUS[23] value of $b = 5.1 \pm 1.1(\text{stat.}) \pm 0.7(\text{syst.})$ GeV^{-2} for the range $2 < Q^2 < 40$ GeV^2, $55 < W < 125$ GeV. The fits, carried out in the $|t|$ region below 1 GeV^2, are consistent with a single exponential for the elastic t distribution in both experiments. The statistical accuracy of the J/ψ electroproduction data do not yet allow for a determination of b as function of W to test shrinkage.

Note that the slope parameter $b(J/\psi)$ for elastic J/ψ production (average $Q^2 \approx 8$ GeV^2) is substantially smaller than the one for light vector mesons: For elastic ρ production[23,26] at a similar Q^2, e.g., the value $b(\rho) \approx 8$ GeV^{-2} is found. This behavior is qualitatively explained in the optical picture of scattering, where the b parameter can be viewed as the sum of the scattering partner's radii squared: $b \approx R_p^2 + R_V^2$. Due to the large mass of the charm quarks their velocities in a J/ψ bound state is small as is, as a consequence of the uncertainty principle, the J/ψ radius. The slope b is therefore given mainly by the (larger) radius of the proton, which is composed of light quarks. On the basis of this it is expected that the b slope for elastic Υ production will be similar to the one for the J/ψ.

Compared to elastic production, the b slopes for J/ψ production with proton dissociation are smaller[22,31] by typically a factor of 2, both for heavy and light vector mesons. Again the "optical" picture provides a qualitative understanding: The elastic scattering is a coherent effect involving the entire proton, while the dissociative process is thought to proceed as quasi-elastic scattering off the ("smaller") constituent quarks in the proton[32].

Helicity analysis: In order to disentangle the longitudinal and transverse virtual photon components in exclusive vector meson production, the helicity structure of the interaction can be investigated. This is usually done in the s-channel helicity frame, where the meson emission direction in the $\gamma^* p$ rest system serves as the quantization axis. At given values for W and Q^2 the exclusive production and decay of a meson $V \to l^+ l^-$ is described by three angles: θ^* and ϕ, the polar and azimuthal angles of the positively charged lepton in the V rest system, and the angle Φ between the production plane of the meson V and the electron scattering plane. The probability distribution of these three angles can be expressed by the spin density matrix elements or linear combinations of these (see, e.g., [33]). Assuming s-channel helicity conservation (SCHC), the number of independent angles reduces to two, where the polarization angle $\Psi = \phi - \Phi$ absorbs one degree of freedom. The two remaining angular distributions depend on the matrix elements (bilinear combinations of the helicity amplitudes) r_{00}^{04} and $r_{1,-1}^{1}$, where the lower indices denote the helicities of the vector meson in the bilinear combination and the upper indices are conventional[33] and refer to the photon helicity producing the vector meson. Integrating over the other respective angle, the following distributions are obtained:

$$\frac{d\sigma}{d\cos\theta^*} \propto 1 + r_{00}^{04} + \left(1 - 3r_{00}^{04}\right)\cos^2\theta^* \tag{12}$$

$$\frac{d\sigma}{d\Psi} \propto 1 - \epsilon\, r_{1-1}^{1} \cos 2\Psi \ . \tag{13}$$

The acceptance corrected distributions from recent H1 measurements[21] of $\cos\theta^*$ and Ψ are shown in fig. 8 for two ranges of Q^2. The $\cos\theta^*$ distribution nicely supports the expectation of a dominating longitudinal photon polarization as Q^2 is increased: Fits to the data from H1[21] yield the values $r_{00}^{04} = 0.15 \pm 0.11$ at $\langle Q^2 \rangle = 4$ GeV^2 and $r_{00}^{04} = 0.48 \pm 0.15$ at $\langle Q^2 \rangle = 16$ GeV^2, suggesting that the longitudinal component of the J/ψ indeed increases with Q^2. The Ψ distributions

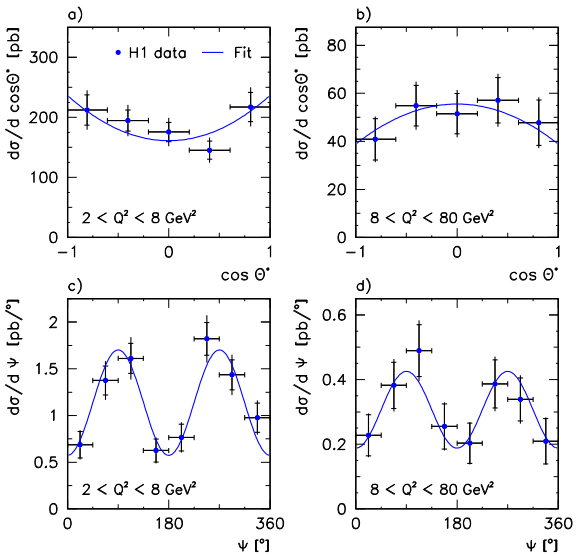

Fig. 8. Distributions of $\cos\theta^*$ (a) and b)) and of Ψ (c) and d)) for the positive lepton from J/ψ decay from the quasi-elastic (elastic plus proton-dissociative) process $ep \to eJ/\psi X$ in the range $40 < W < 160$ GeV, for two intervals in Q^2 from H1[21]. The inner error bars indicate statistical, the outer error bars statistical and systematic errors added in quadrature. The lines are the results of fits described in the text.

provide measurements of $r^1_{1-1} = 0.50 \pm 0.08$ at $\langle Q^2 \rangle = 4$ GeV^2 and $r^1_{1-1} = 0.39 \pm 0.13$ at $\langle Q^2 \rangle = 16$ GeV^2. Assuming natural parity exchange (NPE), the two matrix elements are related by $r^1_{1-1} = \frac{1}{2}(1 - r^{04}_{00})$. Using this relation and the measured values for r^{04}_{00} one obtains agreement within one standard deviation with the direct measurement of r^1_{1-1} from the Ψ distributions. Thus both SCHC and NPE are hypotheses supported by the elastic J/ψ production data at HERA.

Assuming SCHC to hold, the measurements of r^{04}_{00} can be used to determine the ratio R of longitudinal to transverse virtual photon cross sections:

$$R = \frac{\sigma_L}{\sigma_T} = \frac{1}{\epsilon} \frac{r^{04}_{00}}{1 - r^{04}_{00}} \ . \tag{14}$$

For the two Q^2 regions H1 obtain the results $R = 0.18^{+0.18}_{-0.14}$ at $\langle Q^2 \rangle = 4$ GeV^2 and $R = 0.94^{+0.79}_{-0.43}$ at $\langle Q^2 \rangle = 16$ GeV^2, compatible with the ZEUS result[23] of $R = 0.41^{+0.45}_{-0.52}$ at $\langle Q^2 \rangle = 5.9$ GeV^2. Together with the photoproduction data (see below) the measurements suggest a rise of R, i.e. an increase of the fraction of longitudinally polarized virtual photons, with Q^2.

Within the above-mentioned pQCD models, R is approximately proportional to Q^2/M_V^2. This relation can be tested comparing ρ with J/ψ production with the result that the value for $R(\rho)$ from elastic ρ production is found to be significantly larger[23,26] than $R(J/\psi)$ from elastic J/ψ production. But $R(\rho)$ and $R(J/\psi)$ are of the same order, when the value of Q^2 is reduced appropriately in elastic ρ production to match the values of Q^2/M_V^2 in both reactions.

4.3 Electroproduction of ψ'(2S) Mesons

H1[21] has observed quasi-elastic production of $\psi(2S)$ in deep inelastic scattering using the decay channel $\psi(2S) \to J/\psi\ \pi^+\pi^-$. No separation of elastic and proton dissociation was possible due to reasons of lacking statistics. Qualitatively, the cross section ratio $\sigma(\psi(2S))/\sigma(J/\psi)$ is expected to be significantly smaller than unity due to the smaller wave function at the origin for the $\psi(2S)$ particle ($1^{\rm st}$ radial excitation) compared to the J/ψ. Within the Q^2 range from 1 to 80 GeV^2 the cross section ratio $\sigma(\psi(2S))/\sigma(J/\psi)$ was determined and compared to pQCD models[14,34], which predict a rise of this ratio from ≈ 0.2 (photoproduction, see below) to ≈ 0.4 for large Q^2 ($Q^2 \gg M_V^2$), in agreement with the measurements.

5 Photoproduction of Heavy Quarkonia

Diffractive photoproduction is one of the classical domains for the successful application of Regge theory. Perturbative QCD calculations, on the other hand, are deprived of their "natural" scale Q^2 and cannot be applied here in the usual way, since in photoproduction the photon virtuality does not provide a hard scale. However, due to the Q^2 effect in the emission of photons from the incoming electron or positron suppressing high virtualities, photoproduction events are more abundant at HERA compared to deep inelastically produced events, allowing for selection of data exhibiting an alternative hard scale. In vector meson photoproduction, the mass of a produced heavy quarkonium state and/or the momentum transfer at the proton vertex may serve as such scales. For inelastic reactions, mediated dominantly by photon-gluon fusion, Regge theory cannot be applied but full next-to-leading order (NLO) QCD calculations exist[35].

5.1 Inelastic Photoproduction of Charmonium

Both H1[36] and ZEUS[37] have recently presented analyses on inelastic production of J/ψ in the photoproduction limit. The inelastic component was extracted by a cut in z: ZEUS use $0.55 < z < 0.9$ with a W range of $50 < W < 180$ GeV, while H1 selects $0.3 < z < 0.9$ and $60 < W < 180$ GeV. The data are corrected for the lower z cuts using Monte Carlo techniques. The differential cross sections $d\sigma/dz$ for both experiments (not shown) are well described by the color singlet model in NLO, but are not compatible with a leading order color octet model, as found in the ZEUS analysis. It has been pointed out[38], however, that the theoretical calculations contain considerable uncertainties, so that the color octet model based on the framework on NRQCD[17] cannot be ruled out by the HERA data. This should be compared with the conclusions from the electroproduction data (see above), where the leading order color singlet model was not sufficient to describe the measurements, but, due to missing NLO predictions, octet contributions could still not be claimed.

The ratio of the inelastic $\psi(2S)$ over J/ψ photoproduction cross section was remeasured recently by H1[36] and ZEUS[39] at photon proton center of

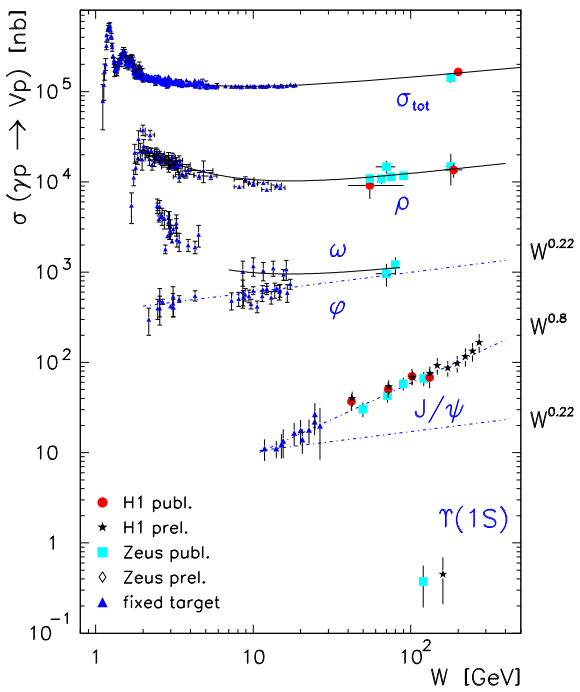

Fig. 9. Data on the total photoproduction cross section and cross sections for elastic vector meson production as function of the photon-proton center of mass energy W, for fixed target experiments and from the HERA collider. The cross sections for light vector mesons $V = \rho, \omega, \phi$ are well described by the soft Pomeron model, while J/ψ cross sections are rising much steeper with W. Statistics for Υ production is not yet sufficient to determine the W dependence of the cross section at HERA.

mass energies $60 < W < 180$ GeV (H1) and $50 < W < 180$ GeV (ZEUS). H1 finds the cross section ratio to be 0.21 ± 0.06 (the error contains statistical and systematic uncertainties), in good agreement with the ZEUS value of $0.242 \pm 0.065(\text{stat.})\,^{+0}_{-0.019}(\text{syst.})$. Comparing to similar measurements from fixed target experiments at typical energies $W \approx 10$ GeV, no dependence of this ratio on W can be observed within the large uncertainties.

5.2 Exclusive Photoproduction of J/ψ Mesons

The total cross section for elastic photoproduction of light vector mesons, $\gamma p \to Vp$, $V = \rho, \omega, \phi$, is well described within the Regge model by soft Pomeron exchange (see, e.g. [27]), predicting a universal, weak dependence $\sigma \sim W^{0.22}$. This model, however, cannot accommodate heavy vector meson photoproduction ($V = J/\psi, \psi(2S), \Upsilon$), as clearly established with the HERA data [40–45] shown in fig. 9. Fitting the J/ψ cross section to the form $\sigma \sim W^{\delta}$ yields $\delta \approx 0.80$, resulting from a much steeper rise of the cross section with increasing W compared to the universal expectation.

As is discussed in more detail elsewhere[27], the electroproduction cross sections for the light vector mesons also start to rise faster with W than the soft expectation , when the photon virtuality Q^2 approaches a "hard" scale, typically 10 GeV^2. The fact that the total cross section of elastic photoproduction of J/ψ mesons shows already "hard" behavior suggests that the hard scale is provided

by the mass of the heavy vector meson itself ($M^2_{J/\psi} \sim 10$ GeV^2): Perturbative QCD can be applied to the deep inelastic and to the photoproduction processes, since the relevant scale $\tilde{Q}^2$ for these processes can be written[13] as

$$\tilde{Q}^2 = \frac{Q^2 + M_V^2}{4} \,, \tag{15}$$

which is much larger than $\Lambda_{\rm QCD}$, even for photoproduction ($Q^2 = 0$) of heavy vector mesons such as the J/ψ.

Figure 10 shows the cross section $\gamma p \to J/\psi\, p$ from the fixed target experiments[46,47] and the results from ZEUS[41] and H1[40,42] together with the leading order pQCD predictions of Frankfurt et al.[15], using various parameterizations of the gluon distribution inside the proton, such as GRV(HO)[28], MRSR2[29], and CTEQ4M[48]. Note the large W range of the preliminary H1 data[42], reaching up to $W = 285$ GeV, close to the kinematic limit of HERA (300 GeV). These measurements have become possible through the use of a novel hardware trigger system at level 2, based on the neural network architecture[49].

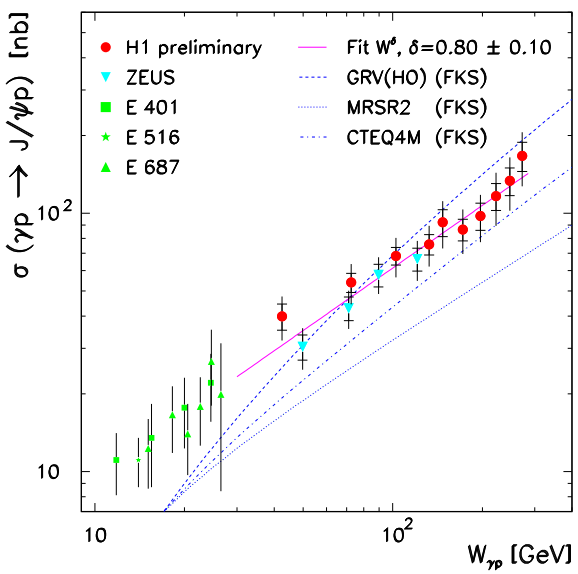

Fig. 10. Total cross section for elastic photoproduction of J/ψ mesons from HERA[40–42] and fixed target experiments[46,47]. The power law fit shown (full line) is for the HERA data alone. The curves are from a pQCD model[15] using various assumptions of the gluon density (see text). The absolute normalization of the pQCD predictions strongly depends on the mass of the charmed quark. Note that these models predict a "convex" shape in this $\log\sigma$ vs $\log W$ representation.

While there is a large uncertainty in the absolute value of the prediction, depending strongly on the charm quark mass (see also fig. 6), the W dependence is a "hard" prediction from pQCD: The slope of the data is best described using MRSR2 or CTEQ4, while GRV(HO) is slightly too steep. Fitting a power law ($\sigma \sim W^\delta$) to the combined HERA and fixed target data yields[50] $\delta = 0.83 \pm 0.05$, much steeper than the prediction of the Donnachie and Landshoff model using the soft Pomeron ($\delta \approx 0.22 - 0.32$). A phenomenological solution to

this problem was offered by Donnachie and Landshoff[11], introducing a second, "hard", Pomeron trajectory $\alpha_{\mathrm{P}'}(t) = 1.4 + 0.1t$. This trajectory exhibits a much stronger W rise (the intercept $\alpha_{\mathrm{P}'}(0) = 1.4$, as opposed to 1.08 from the soft Pomeron), and a much reduced W dependence of the b parameter ($\alpha'_{\mathrm{P}'} = 0.1$ instead of 0.25 GeV^{-2} for the soft Pomeron). A two-Pomeron fit, adjusting the relative contributions of the two Pomerons, is able to describe the data[50]. A distinctive feature of the two-Pomeron model as opposed to the pQCD prediction is its W dependence: While the pQCD model suggests a "convex" shape in the representation $\log\sigma$ vs $\log W$ (see fig. 10), the two-Pomeron model predicts a "concave" shape with an accelerated rise at the end of the HERA kinematic range. Within the present experimental accuracy, neither of the two shapes can be excluded.

t distribution: For photoproduction, the momentum transfer t at the proton vertex can be approximated by the transverse momentum squared, p_T^2, of the J/ψ. The p_T^2-distribution can then be used to fit an exponential $\exp(-b|t|)$ for low values of $|t|$ (typically $|t| < 1$ GeV^2). The resulting b parameters are very close to the ones obtained from electroproduction: H1[50], e.g., find a value of $b = 4.2 \pm 0.2(\mathrm{stat.}) \pm 0.6(\mathrm{syst.})$, in good agreement with the result from ZEUS[51], $b = 4.6 \pm 0.4(\mathrm{stat.})^{+0.4}_{-0.6}(\mathrm{syst.})$. Statistics in photoproduction is larger than in electroproduction so that the W dependence of the slope parameter can be studied[50]: In the range $40 < W < 150$ GeV five W bins were created and $b(W)$ was parameterized according to eq. 4, where the shrinkage parameter α'_{P} was allowed to freely vary in the fit. The result of the fit to the entire W range is

$$b = (4.5 \pm 0.2) + 4 \cdot (0.18 \pm 0.09) \cdot \ln\left(\frac{W}{90\mathrm{GeV}}\right) \left[\mathrm{GeV}^{-2}\right] . \qquad (16)$$

Shrinkage due to the soft Pomeron model demands $\alpha'_{\mathrm{P}} = 0.25$, compared to 0.18 ± 0.09 from the fit. While the data are clearly compatible with being independent of W, shrinkage cannot be excluded within the present uncertainties.

5.3 Photoproduction of Υ Mesons

An even larger scale in the process $\gamma p \to Vp$ is provided when Υ mesons are produced ($V = \Upsilon$). The naive expectation would suggest a rise of the cross section with W, even steeper than for the J/ψ, driven by the gluon density in the proton which becomes larger as x_g decreases and the relevant scale $\tilde{Q}$ (here the mass of the vector meson V) increases. Both ZEUS[52] and H1[53] have observed photoproduction of Υ mesons, decaying into μ pairs. Due to limited mass resolution, the three radial excitations $\Upsilon(1S), \Upsilon(2S)$ and $\Upsilon(3S)$ cannot be resolved. The main source of background is the non-resonant Bethe-Heitler process, which is subtracted statistically. Experimentally, the sum of the products of the elastic $\Upsilon(iS)$ photoproduction cross sections and their respective branching ratios B_i into $\mu^+\mu^-$ is determined. ZEUS obtain $13.3 \pm 6.0(\mathrm{stat.})^{+2.7}_{-2.3}(\mathrm{syst.})$ pb at a mean center of mass energy of 120 GeV, the preliminary value of H1 is

$16 \pm 8(\text{stat.}) \pm 4(\text{syst.})$ pb at a mean center of mass energy of 160 GeV. Both values are in mutual agreement and are well described by a QCD model of Martin et al.[54], using parton-hadron duality. Since Υ photoproduction is reduced by a factor of about 400 relative to the J/ψ (suppressed by $(M_{J/\psi}/M_\Upsilon)^5$, see eq. 6), it is not surprising that statistics is not yet sufficient to study the W dependence of the Υ cross section.

5.4 Photoproduction at High Momentum Transfers

Diffractive processes are characterized by an exponential t dependence, $\sigma/dt \sim e^{-b|t|}$. Most of the above discussions concentrated on elastic processes, exhibiting a steeply falling t behavior and therefore limiting the $|t|$ reach to below ~ 1 GeV^2. When scattering to larger $|t|$ values is considered, an additional hard scale is introduced and improved QCD calculations become possible[55,56]. Calculations concentrating on high momentum transfers can be applied also to the lighter vector mesons.

When $|t|$ is large, the diffractive proton dissociation process is expected to dominate, where a gluon ladder described by the BFKL formalism[57] can be exchanged and predictions can be made for both the t and W dependences[55,56].

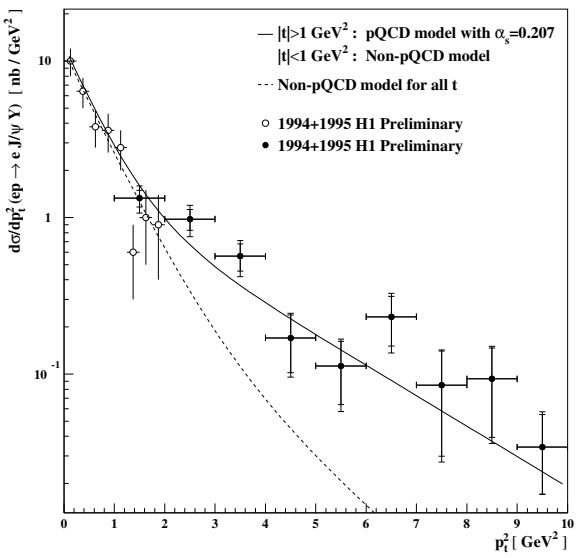

Fig. 11. Differential cross section for J/ψ photoproduction with proton dissociation, as measured by H1[58] (full symbols). The open points are taken from [6], where $Q^2 < 4$ GeV^2. The solid line represents the combination of a pQCD calculation[56] for $|t| > 1$ GeV^2 and a non-perturbative model when $|t| < 1$ GeV^2. The normalization was determined using the measured cross section for $|t| > 1$ GeV^2. The dashed line represents the prediction from the non-perturbative model when the full kinematic range is used.

Both H1[58] and ZEUS[59] have studied quasi-elastic J/ψ photoproduction at large $|t|$. As in the elastic case, the $|t|$ distribution is obtained from the measured p_T^2 of the final state J/ψ, where $t = -p_T^2$ holds to a very good approximation. As an example, the differential cross section $d\sigma/dt$ for J/ψ photoproduction with

proton dissociation from H1 is shown in fig. 11(full symbols), the open points are from elastic photoproduction[6]. Both sets of data are restricted to the kinematic range $30 < W < 150$ GeV. A clear decrease of the slope with increasing p_T^2 is observed. The solid line in the figure is the result of a pQCD calculation[56] in the region $|t| > 1$ GeV^2, using a non-perturbative model for $|t| < 1$ GeV^2. The prediction agrees well with the data, implying that the pQCD calculation describes correctly the large $|t|$ behavior.

According to the expectations from perturbative QCD, the diffractive photoproduction of vector mesons at a hard scale should be, to a good approximation, flavor-independent and proportional to the electromagnetic coupling of the photon to the mesonic $q\bar{q}$ state. In a ZEUS analysis[59] the large $|t|$ behavior in photoproduction also of the light vector mesons (ρ, ϕ) has been studied. It is found that the cross section ratios $\sigma(J/\psi)/\sigma(\rho)$ and $\sigma(\phi)/\sigma(\rho)$ approach their quark model limits 8:9 and 2:9, respectively, as $|t|$ increases. These results also suggest that $|t|$, just like Q^2 and M_V, can play the role of a hard scale, enabling perturbative QCD calculations. A combination of all the three relevant scales may provide an interesting hard scale $\tilde{Q}^2$: It has in fact been suggested[13] earlier, although limited to heavy quarkonia (J/ψ) production, to use the combined scale $\tilde{Q}^2 = (Q^2 + M_V^2 + |t|)/4$. From the present HERA data it seems that such a restriction to heavy quarkonia may not be necessary.

6 Conclusions

HERA has provided a wealth of precise data on electro- and photoproduction of heavy quarkonia, giving access to the rich field of diffractive phenomena in ep collisions. While the diffractive processes involving light vector mesons (ρ, ω, ϕ) show the typical "soft" behavior, i.e. weak dependence of the cross section on W, well described by Pomeron exchange, the corresponding cross sections for heavy quarkonia (J/ψ) exhibit a steep rise with W, incompatible with the soft picture. Another prediction of the soft Pomeron model , i.e. shrinkage of the differential cross section, cannot be seriously tested with heavy quarkonia at present due to lack of statistics.

The W dependence of the cross sections $\sigma(\gamma^{(*)}p \to Vp, V = J/\psi, \Upsilon)$, however, is explained within pQCD by the steep rise of the gluon density in the proton with decreasing x (= increasing W). Also in contrast to the soft Pomeron model, pQCD does not expect shrinkage of the differential cross section. The hard scale necessary to justify pQCD is apparently provided by the mass of the heavy vector meson. This view is beautifully supported by diffractive photoproduction of J/ψ, where pQCD can successfully describe the observed cross sections, the J/ψ mass being the only hard scale in the reaction.

While the soft, single Pomeron model is unable to account for the cross section rise in heavy quarkonium production, models with an additional "hard" Pomeron (two new parameters which need adjustment, plus the relative strength of the two Pomeron components) are able to describe the HERA data again. Also the question of shrinkage, thought to be a distinctive feature, loses its

importance: The hard Pomeron parameters suggest a largely reduced shrinkage effect. As a consequence many of the salient features distinguishing Regge models from pQCD predictions need largely improved statistics, such as shrinkage, the exact shape of the cross section as function of W ("convex" or "concave"), or the open question of SCHC. Future running at HERA with high luminosity will significantly improve the precision of the data.

For future comparisons of theoretical models with, hopefully, statistically improved data one should keep in mind that many of the pQCD predictions for heavy quarkonium production at present are available only in leading order, thus precluding serious confrontation with experiment. One such example is the inelastic production of J/ψ mesons, where the size of possible color octet contributions, apparently necessary for the Tevatron data, cannot yet be quantified in ep collisions: For photoproduction, the NLO color singlet calculation is able to describe the differential cross section $d\sigma/dz$. Additional leading order color octet contributions, especially at high z, would largely exceed the data. But a suppression of such additional color octet contributions in higher order, then being in agreement with the HERA data, is not excluded. On the other hand for electroproduction only the LO color singlet and octet calculations are available. Here, the color singlet prediction alone clearly undershoots the data. Due to a lacking NLO calculation, however, one cannot use this observed discrepancy to claim the necessity of additional octet contributions.

To reach a more complete theoretical understanding along with the expected improvement of the experimental results would be highly desirable: One of the main motivations for studying heavy vector meson production in ep collisions is the possibility to directly extract the gluon density in the proton. This important additional information from the heavy vector meson sector has yet to be supplied and would nicely complement other analyses on the gluonic structure of the nucleon.

Acknowledgments

I am indebted to the organizers for this very pleasant meeting. I would like to thank my colleague Beate Naroska for a critical reading of the manuscript and many helpful suggestions.

References

1. H1 Collaboration: T. Ahmed et al., Nucl. Phys. B439 (1995) 471.
2. ZEUS Collaboration: M. Derrick et al., Z. Phys. C65 (1995) 379.
3. H1 Collaboration: T. Ahmed et al., Nucl. Phys. B429 (1994) 477.
4. ZEUS Collaboration: M. Derrick et al., Phys. Lett. B315 (1993) 481.
5. ZEUS Collaboration: M. Derrick et al., Phys. Lett. B350 (1995) 120.
6. H1 Collaboration: S. Aid et al., Nucl.Phys. B472 (1996) 3.
7. H. Jung, G. A. Schuler and J. Terron, Int. Jour. of Mod. Phys. A7 (1992) 7955.
8. A. Donnachie and P.V. Landshoff, Phys. Lett. B296 (1992) 227.

9. T. Regge, Nuovo Cim. 14 (1959) 951; J.J. Sakurai, Ann. Phys. 11 (1960) 1; see also P.D.B. Collins: An Introduction to Regge Theory and High Energy Physics (Cambridge University Press, 1977).
10. J.J. Sakurai, Phys. Rev. Lett. 22 (1969) 981; H. Fraas and D. Schildknecht, Nucl. Phys. B14 (1969) 543.
11. A. Donnachie and P.V. Landshoff, Phys. Lett. B437 (1998) 408.
12. S.J. Brodsky et al., Phys. Rev. D50 (1994) 3134.
13. M.G. Ryskin, Z. Phys. C57 (1993) 89.
14. L. Frankfurt, W. Koepf and M. Strikman, Phys. Rev. D54 (1996) 3194.
15. L. Frankfurt, W. Koepf and M. Strikman, Phys. Rev. D57 (1998) 512.
16. M.G. Ryskin, R.G. Roberts, A.D. Martin and E.M. Levin, Z. Phys. C76 (1997) 231.
17. G.T. Bodwin, E. Braaten and G.P. Lepage, Phys. Rev. D51 (1995) 1125.
18. S. Fleming and T. Mehen, Phys. Rev. D57 (1998) 1846.
19. G.A. Schuler, CERN-TH-7170-94, hep-ph/9403387.
20. CDF Collaboration: F. Abe et al., Phys. Rev. Lett. 69 (1992) 3704; D0 Collaboration: S. Abachi et al., Phys. Lett. B370 (1996) 239; CDF Collaboration: F. Abe et al., Phys. Rev. Lett. 79 (1997) 572.
21. H1 Collaboration: C. Adloff et el., Eur. Phys. J. C10 (1999) 373.
22. A. Meyer: PhD Thesis, University of Hamburg, 1998.
23. ZEUS Collaboration: J. Breitweg et al., Eur. Phys. J. C6 (1999) 603.
24. G. Ingelman, J. Rathsman and G.A. Schuler, Comp. Phys. Comm. 101 (1997) 135.
25. L.N. Hand, Phys. Rev. 129 (1963) 1834.
26. H1 Collaboration: C. Adloff et al., DESY-99-010, to appear in Eur.Phys.J. C.
27. see also A. Proskuryakov: Experimental Results on the Production of Light Vector Mesons, these proceedings.
28. M. Glück, E. Reya and A. Vogt, Z. Phys. C67 (1995) 433.
29. A.D. Martin, R.G. Roberts and W.J. Stirling, Phys. Lett. B387 (1996) 419.
30. H1 Collaboration: C. Adloff et al., Z. Phys. C75 (1997) 607.
31. H1 Collaboration: Comparison of Elastic and Proton Dissociative ρ Meson Electroproduction from H1, contributed paper 157n to the International Europhysics Conference on High Energy Physics HEP99, Tampere, Finland, July 1999.
32. S.P. Misra, A.R. Panda and B.K. Parida, Phys. Rev. D22 (1980) 1574.
33. K. Schilling and G. Wolf, Nucl. Phys. B61 (1973) 381.
34. J. Nemchik et al., Phys. Lett. B341 (1994) 228 and J. Exp. Theor. Phys. 86 (1998) 1054.
35. M. Krämer et al., Phys. Lett. B348 (1995) 657; M. Krämer, Nucl. Phys. B459 (1996) 3.
36. H1 Collaboration: Inelastic Photoproduction of J/ψ and $\psi(2S)$ at H1, contributed paper 157aj to the International Europhysics Conference on High Energy Physics HEP99, Tampere, Finland, July 1999.
37. ZEUS Collaboration: Measurement of Inelastic J/ψ Photoproduction at HERA, contributed paper 814 to the XXIX International Conference on High Energy Physics ICHEP98, Vancouver, Canada, July 1998.
38. M. Beneke and M. Krämer, Phys. Rev. D55 (1997) 5269; B.A. Kniehl and G. Kramer, Phys. Rev. D56 (1997) 5820; B.A. Kniehl and G. Kramer, Phys. Lett. B413 (1997) 416; M. Beneke, I.Z. Rothstein and M.B. Wise, Phys. Lett. B408 (1997) 373.
39. ZEUS Collaboration: Inelastic Charmonium Photoproduction at HERA, contributed paper 504 to the International Europhysics Conference on High Energy Physics HEP99, Tampere, Finland, July 1999.

40. H1 Collaboration: S. Aid et al., Nucl. Phys. B468 (1996) 3.
41. ZEUS Collaboration: J. Breitweg et al., Z. Phys. C75 (1997) 215.
42. H1 Collaboration: C. Adloff et al.: Elastic Production of J/ψ Mesons in Photoproduction and at High Q^2 at HERA, contributed paper 242 to the International Europhysics Conference on High Energy Physics HEP97, Jerusalem, August 1997.
43. ZEUS Collaboration, J. Breitweg et al.: Exclusive Vector Meson Production in Deep Inelastic Scattering at HERA, contributed paper 639 to the International Europhysics Conference on High Energy Physics HEP97, Jerusalem, August 1997.
44. H1 Collaboration: C. Adloff et al., Phys. Lett. B421 (1998) 385.
45. ZEUS Collaboration: J. Breitweg et al., Z. Phys. C76 (1997) 599.
46. E401 Collaboration: M. Brinkley et al., Phys. Rev. Lett. 48 (1982) 73.
47. E516 Collaboration: B.H. Denby et al., Phys. Rev. Lett. 52 (1984) 795.
48. H.L.Lai et al., Phys. Rev. D55 (1997) 1280.
49. J.H. Köhne et al., Realization of a second level neural network trigger for the H1 experiment at HERA, Nucl. Inst. Meth. A389 (1997) 128.
50. H1 Collaboration: Diffractive J/ψ Production, contributed paper 157aj to the International Europhysics Conference on High Energy Physics HEP99, Tampere, Finland, July 1999.
51. ZEUS Collaboration: J. Breitweg et al., kZ. Phys. C75 (1997) 215.
52. ZEUS Collaboration: J. Breitweg et al., Phys. Lett. B437 (1998) 432.
53. H1 Collaboration: Observation of Υ Production at HERA, contributed paper 574 to the XXIX International Conference on High Energy Physics ICHEP98, Vancouver, Canada, July 1998.
54. A.D. Martin, M.G. Ryskin and T. Teubner, Phys. Lett. B454 (1999) 339.
55. J.R. Forshaw and M.G. Ryskin, Z. Phys. C68 (1995) 137.
56. J. Bartels, J.R. Forshaw, H. Lotter and M. Wüsthoff, Phys. Lett. B375 (1996) 301.
57. S.J. Brodsky et al., JETP Lett. 70 (1999) 155.
58. H1 Collaboration: Production of J/ψ Mesons with large $|t|$ at HERA, contributed paper 274 to the International Europhysics Conference on High Energy Physics HEP97, Jerusalem, August 1997.
59. ZEUS Collaboration: Study of Vector Meson Production at Large $|t|$ at HERA and Determination of the Pomeron Trajectory, contributed paper 788 to the XXIX International Conference on High Energy Physics ICHEP98, Vancouver, Canada, July 1998.